*Inorg. Chem.* **2003**, *42*, 1107–1111

# A Novel Hexanuclear Mixed Oxidation State $Cu^{II}_4Cu^{I}_2$ Cluster Complex Exhibiting Weak Ferromagnetic Exchange

**Zhiqiang Xu, Laurence K. Thompson,* and David O. Miller**

*Department of Chemistry, Memorial University of Newfoundland, St. John's, Newfoundland A1B 3X7, Canada*

**Eliseo Ruiz and Santiago Alvarez***

*Departament de Química Inorgànica, Universitat de Barcelona, Diagonal 647, 08028 Barcelona, Spain*

Received July 16, 2002

The complex $[(PAH)_4Cu^{II}_4Cu^{I}_2Br_{10}]$ (**1**) (PAH = picolinamide hydrazone) containing a $Cu^{II}_4Cu^{I}_2$ hexanuclear cluster, with two well-separated $Cu^{II}_2$ dinuclear centers, results from a redox reaction involving a hydrolytically unstable ligand, salicilyl picolinamide hydrazone, and $CuBr_2$ in aqueous acetonitrile. The $Cu^{II}$ centers are axially bridged via long bromine contacts, leading to ferromagnetic exchange ($2J = 4.04$ cm$^{-1}$). Density functional calculations have been carried out, giving a comparable singlet–triplet splitting energy. **1** crystallizes in the triclinic system, space group $P\bar{1}$, with $a = 9.253(3)$ Å, $b = 18.159(3)$ Å, $c = 7.199(5)$ Å, $\alpha = 91.31(3)°$, $\beta = 107.35(4)°$, $\gamma = 104.22(2)°$, and $Z = 2$.

## Introduction

Mixed oxidation state ($Cu^{II}/Cu^{I}$) polycopper clusters are an interesting class of compounds with relevance to both biochemistry and inorganic chemistry, and a few examples of localized (class II,[1] e.g., $[Cu_3Cl_6]^{2-}$ and $[Cu_4Br_{10}]^{4-}$)[2,3] and delocalized (class III,[1] e.g., $[Cu_2Br_5]^{2-}$ and $[Cu_8Br_{15}]^{6-}$)[4,5] systems are known. The latter case involves two cubane-like $Cu_4Br_7$ clusters linked by a single bromine bridge. ESR data suggest complete delocalization of the $Cu^{II}$ unpaired electron over all eight copper centers. No magnetic data have been reported. Frequently the mixed oxidation state species are produced by a sacrificial redox reaction involving a benign reducing agent, e.g., Cu metal, which acts as a reducing agent,[4] or by mixing $Cu^{II}$ and $Cu^{I}$ salts in an appropriate ratio.[4,5]

Exchange coupling in such systems is clearly limited, since in most examples there is only one $Cu^{II}$ center. The present paper highlights a special case where a neutral mixed oxidation state complex results from a redox reaction involving a hydrolytically unstable ligand, salicilyl picolinamide hydrazone (PTS), and $CuBr_2$ in aqueous acetonitrile. Ligand hydrolysis during the reaction leads to $[(PAH)_4Cu^{II}_4Cu^{I}_2Br_{10}]$ (PAH = picolinamide hydrazone), containing a $Cu^{II}_4Cu^{I}_2$ hexanuclear cluster, with two separate $Cu^{II}_2$ dinuclear centers which are ferromagnetically coupled. Density functional calculations have been carried out to complement the characterization of the magnetic structure of this compound.

## Experimental Section

**Physical Measurements**. Electronic spectra were recorded as Nujol mulls with a Cary 5E spectrometer. Infrared spectra were recorded as Nujol mulls using a Mattson Polaris FTIR instrument. C, H, N analyses on a vacuum-dried sample were carried out by the Canadian Microanalytical Service, Delta, British Columbia, Canada. Variable-temperature magnetic data (2−300 K) were obtained with a Quantum Design MPMS5S Squid magnetometer operating at 0.1−5.0 T. Calibrations were carried out with a palladium standard cylinder, and temperature errors were assessed with $[H_2TMEN][CuCl_4]$ ($H_2TMEN = (CH_3)_2HNCH_2CH_2NH(CH_3)^{2+}$).[6]

* Authors to whom correspondence should be addressed. E-mail: lthomp@mun.ca (L.K.T.); Santiago@qi.ub.es (S.A.). Fax: 1-709-737-3702 (L.K.T.); 34-93-4907725 (S.A.).

(1) Robin, M. B.; Day, P. *Adv. Inorg. Chem. Radiochem.* **1967**, *10*, 247.
(2) Willett, R. D.; Halvorson, K. *Acta Crystallogr., Part C* **1988**, *44*, 2068.
(3) Scott, B.; Willett, R. D. *Inorg. Chem.* **1991**, *30*, 110.
(4) Horn, C.; Dance, I. G.; Craig, D.; Scudder, M. L.; Bowmaker, G. A. *J. Am. Chem. Soc*. **1998**, *120*, 10549.
(5) Bowmaker, G. A.; Boyd, P. D. W.; Rickard, C. E. F.; Scudder, M. L.; Dance, I. G. *Inorg. Chem.* **1999**, *38*, 5476.

10.1021/ic0204631 CCC: $25.00 
Published on Web 01/23/2003

**Table 1.** Crystallographic Data for **1**

| | | | |
|---|---|---|---|
| empirical formula | $C_{12}H_{16}Br_5Cu_3N_8$ | $\gamma$ (deg) | 104.22(2) |
| space group | *P*1 | *V* (Å$^3$) | 1113.1(8) |
| fw | 862.47 | Z | 2 |
| *T* (K) | 298(1) | $\lambda$ (Å) | 0.71069 |
| *a* (Å) | 9.253(3) | $\rho_{calcd}$ (g·cm$^{-3}$) | 2.573 |
| *b* (Å) | 18.159(3) | $\mu$ (cm$^{-1}$) | 118.58 |
| *c* (Å) | 7.199(5) | GOF | 1.64 |
| $\alpha$ (deg) | 91.31(3) | R[a] | 0.038 |
| $\beta$ (deg) | 107.35(4) | $R_w$[a] | 0.036 |

[a] $R = \sum||F_o| - |F_c||/\sum|F_o|$; $R_w = [(\sum w(|F_o| - |F_c|)^2\sum wF_o^2)]^{1/2}$.

**Synthesis of PTS**. PTS was synthesized from the reaction of picolinamide hydrazone (PAH) with salicylaldehyde in absolute ethanol by a published procedure,[7,8] and obtained in a pure state.

**Synthesis of $[(PAH)_4Cu^{II}_4Cu^{I}_2Br_{10}]$ (1)**. PTS (0.24 g, 1.0 mmol) was dissolved in acetonitrile (10 mL) and added to a hot solution of $CuBr_2$ (0.45 g, 2.0 mmol) in methanol (20 mL). The resulting dark brown solution was filtered and allowed to stand at room temperature overnight. Dark brown crystals formed, which were filtered off, washed with methanol, and air-dried (yield 0.10 g, 23%). IR (cm$^{-1}$): 3315, 3286 [$\nu(NH_2)$], 1021 (py). UV/vis ($\lambda_{max}$, nm): 465 (CT), 680. Anal. Calcd for $[(C_6H_8N_4)_4Cu_6Br_{10}]$: C, 16.71; H, 1.87; N, 12.99. Found: C, 17.12; H, 2.02; N, 13.15.

**X-ray Crystallography**. The diffraction intensities of a brown, irregular single crystal of **1** were collected with graphite-monochromated Mo K$\alpha$ X-radiation using a Rigaku AFC6S diffractometer at 299(1) K and the $\omega-2\theta$ scan technique. The data were corrected for Lorentz and polarization effects. The structures were solved by direct methods.[9,10] All atoms except hydrogen were refined anisotropically. Hydrogen atoms were optimized by positional refinement, with isotropic thermal parameters set 20% greater than those of their bonded partners at the time of their inclusion. However, they were fixed for the final round of refinement. Neutral atom scattering factors[11] and anomalous-dispersion terms[12,13] were taken from the usual sources. All calculations were performed with the teXsan[14] crystallographic software package using a PC computer. Abbreviated structural details are listed in Table 1.

**Density Functional Calculations**. In recent work we have shown the ability of density functional methods based on the hybrid functional[15] B3LYP to provide accurate numerical estimates of the exchange coupling constant in transition-metal complexes.[16,17] In the B3LYP method the exchange functional calculated using Kohn−Sham orbitals[18] is combined with a generalized gradient approximation (GGA) functional[19,20] by fitting, in the B3LYP case, three mixing parameters to a set of experimental data. We use the B3LYP method as implemented in the GAUSSIAN package[21] combined with a modified broken-symmetry approach using the nonprojected energy of the broken-symmetry solution as the singlet energy.[22] A triple-$\zeta$ basis set has been used for the copper and bromine atoms with (842111/63111/411) and (842111/64111/51) contraction patterns, respectively,[23] while double-$\zeta$ basis sets were employed for the rest of the atoms.[24]

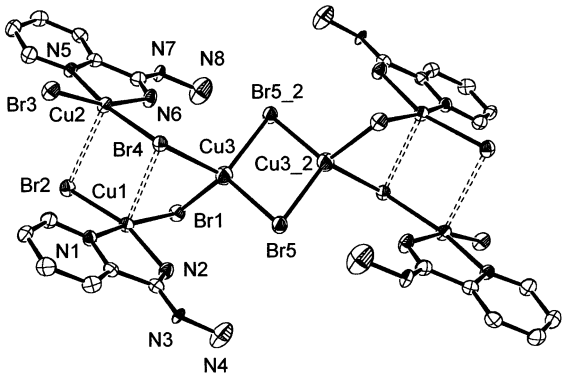


**Figure 1.** Structural representation of **1** (40% thermal ellipsoids).

## Results and Discussion

**Ligand Hydrolysis and the Structure of 1**. The structural representation of **1** is illustrated in Figure 1, and selected bond distances and angles are listed in Table 2. The ligand in the structure is not the same as PTS, and in fact is picolinamide hydrazone, PAH, one of the starting materials used in the ligand synthesis. It is clear that during the reaction between $CuBr_2$ and PTS hydrolysis of the ligand has occurred (Scheme 1), and that part of the $Cu^{II}$ content has been reduced to $Cu^{I}$. The ligand hydrolyis is presumably metal ion assisted, and it seems reasonable to assume that PAH itself could be acting as a sacrificial reducing agent, and that the other hydrolysis product, salicylaldehyde, could also have some reducing capacity. It is of interest to note that the complex $(PTS\text{-}2H)Cu_2(NO_3)_2 \cdot 3.5H_2O$[25] is stable when produced in methanol, with no evidence of ligand decomposition, and

(6) Brown, D. S.; Crawford, V. H.; Hall, J. W.; Hatfield, W. E. *J. Phys. Chem.* **1977**, *81*, 1303.
(7) Case, F. H. *Heterocycl. Chem.* **1970**, *7*, 1001.
(8) Case, F. H. *J. Org. Chem.* **1965**, *30*, 931.
(9) SIR92: Altomare, A.; Cascarano, M.; Giacovazzo, C.; Guagliardi, A. *J. Appl. Crystallogr.* **1993**, *26*, 343.
(10) DIRDIF94: Beurskens, P. T.; Admiraal, G.; Beurskens, G.; Bosman, W. P.; de Gelder, R.; Israel, R.; Smits, J. M. M. *The DIRDIF-94 program system*; Technical Report of the Crystallography Laboratory, University of Nijmegen, The Netherlands.
(11) Cromer, D. T.; Waber, J. T. *International Tables for X-ray Crystallography*; The Kynoch Press: Birmingham, England, 1974; Vol. IV, Table 2.2 A.
(12) Ibers, J. A.; Hamilton, W. C. *Acta Crystallogr.* **1964**, *17*, 781.
(13) Creagh, D. C.; McAuley, W. J. In *International Tables for Crystallography*; Wilson, A. J. C., Ed.; Kluwer Academic Publishers: Boston, 1992; Vol. C, Table 4.2.6.8, pp 219−222.
(14) teXsan for Windows: Crystal Structure Analysis Package, Molecular Structure Corp., Houston, TX, 1997.
(15) Becke, A. D. *J. Chem. Phys.* **1993**, *98*, 5648.
(16) Ruiz, E.; Alemany, P.; Alvarez, S.; Cano, J. *J. Am. Chem. Soc.* **1997**, *119*, 1297.
(17) E. Ruiz, S. Alvarez, A. Rodríguez-Fortea, P. Alemany, Y. Pouillon, C. Massobrio. In *Magnetism: Molecules to Materials*; Miller, J. S., Drillon, M., Eds.; Wiley-VCH: New York, 2001; Vol. 2, Chapter 7, pp 227−279.
(18) Parr, R. G.; Yang, W. *Density-Functional Theory of Atoms and Molecules*; Oxford University Press: New York, 1989.
(19) Becke, A. D. *Phys. Rev. A* **1988**, *38*, 3098.
(20) Lee, C.; Yang, W.; Parr, R. G. *Phys. Rev. B* **1988**, *37*, 785.
(21) Gaussian 98 (Revision A.6): Frisch, M. J.; Trucks, G. W.; Schlegel, H. B.; Scuseria, G. E.; Robb, M. A.; Cheeseman, J. R.; Zakrzewski, V. G.; Montgomery, J. A.; Stratmann, R. E.; Burant, J. C.; Dapprich, S.; Millam, J. M.; Daniels, A. D.; Kudin, K. N.; Strain, M. C.; Farkas, O.; Tomasi, J.; Barone, V.; Cossi, M.; Cammi, R.; Mennucci, B.; Pomelli, C.; Adamo, C.; Clifford, S.; Ochterski, J.; Petersson, G. A.; Ayala, P. Y.; Cui, Q.; Morokuma, K.; Malick, D. K.; Rabuck, A. D.; Raghavachari, K.; Foresman, J. B.; Cioslowski, J.; Ortiz, J. V.; Stefanov, B. B.; Liu, G.; Liashenko, A.; Piskorz, P.; Komaromi, I.; Gomperts, R.; Martin, R. L.; Fox, D. J.; Keith, T.; Al-Laham, M. A.; Peng, C. Y.; Nanayakkara, A.; Gonzalez, C.; Challacombe, M.; Gill, P. M. W.; Johnson, B. G.; Chen, W.; Wong, M. W.; Andres, J. L.; Head-Gordon, M.; Replogle, E. S.; Pople, J. A., Gaussian, Inc, Pittsburgh, PA, 1998.
(22) Ruiz, E.; Cano, J.; Alvarez, S.; Alemany, P. *J. Comput. Chem.* **1999**, *20*, 1391.
(23) Schaefer, A.; Huber, C.; Ahlrichs, R. *J. Chem. Phys.* **1994**, *100*, 5829.
(24) Schaefer, A.; Horn, H.; Ahlrichs, R. *J. Chem. Phys.* **1992**, *97*, 2571.
(25) Xu, Z.; Thompson, L. K. Unpublished results.

**Table 2.** Selected Bond Lengths (Å) and Angles (deg) for **1**

| | | | |
|---|---|---|---|
| Br(1)−Cu(1) | 2.442(2) | Br(5)_2−Cu(3) | 2.467(2) |
| Br(1)−Cu(3) | 2.504(2) | Cu(1)−N(1) | 2.043(6) |
| Br(2)−Cu(1) | 2.389(1) | Cu(1)−N(2) | 1.966(6) |
| Br(3)−Cu(2) | 2.366(2) | Cu(2)−N(5) | 2.046(6) |
| Br(4)−Cu(2) | 2.476(1) | Cu(2)−N(6) | 1.967(7) |
| Br(4)−Cu(3) | 2.571(2) | N(3)−N(4) | 1.439(9) |
| Br(5)−Cu(3) | 2.461(2) | N(7)−N(8) | 1.444(8) |
| Cu(1)−Br(4) | 2.899(5) | Cu(2)−Br(2) | 2.933(4) |
| Cu(2)−Cu(3) | 4.163(1) | Cu(1)−Cu(3) | 3.269(1) |
| Cu(1)−Cu(2) | 3.670(1) | Cu(3)−Cu(3) | 3.082(1) |
| Cu(1)−Br(1)−Cu(3) | 82.74(6) | Cu(2)−Br(4)−Cu(3) | 111.11(5) |
| Cu(3)−Br(5)−Cu(3)_2 | 77.42(5) | Br(1)−Cu(1)−Br(2) | 93.25(5) |
| Br(1)−Cu(1)−N(1) | 171.3(2) | Br(1)−Cu(1)−N(2) | 92.0(2) |
| Br(2)−Cu(1)−N(1) | 95.3(2) | Br(2)−Cu(1)−N(2) | 163.8(2) |
| N(1)−Cu(1)−N(2) | 80.3(3) | Br(3)−Cu(2)−Br(4) | 93.29(5) |
| Br(3)−Cu(2)−N(5) | 94.4(2) | Br(3)−Cu(2)−N(6) | 163.5(2) |
| Br(4)−Cu(2)−N(5) | 170.2(2) | Br(4)−Cu(2)−N(6) | 91.2(2) |
| N(5)−Cu(2)−N(6) | 79.8(3) | Br(1)−Cu(3)−Br(4) | 97.89(6) |
| Br(1)−Cu(3)−Br(5) | 114.38(7) | Br(1)−Cu(3)−Br(5) | 117.59(7) |
| Br(4)−Cu(3)−Br(5) | 115.80(6) | Br(4)−Cu(3)−Br(5) | 109.18(7) |
| Br(5)−Cu(3)−Br(5)_2 | 102.58(5) | | |

**Scheme 1**

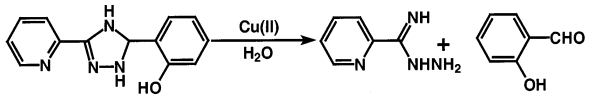


so the presence of acetonitrile and bromide is also considered a factor in the synthesis of **1**. Certainly acetonitrile would enhance the stability of a $Cu^{I}$ species. No other clearly defined products were identified in the reaction mixture.

The structure of **1** is unique, combining four $Cu^{II}$ and two $Cu^{I}$ centers in the same neutral molecule with a $Cu_2Br_6^{4-}$ core, involving two edge-fused pseudotetrahedral $Cu^{I}$ centers (Cu(3)) with a Cu−Cu separation of 3.082(1) Å. Angles at Cu(3) indicate somewhat compressed tetrahedra, with Cu−Br bond distances in the range 2.56−2.57 Å, typical for isolated $Cu^{I}$ cluster anions of this sort.[26] Bromine atoms Br(1) and Br(4) act as bridges and link this core to the external pseudo-square-planar $Cu^{II}$ sites, with a bidentate PAH ligand and a terminal bromine bound to each $Cu^{II}$ center (Cu(1), Cu(2)). Typical in-plane Cu−ligand distances are found for Cu(1) and Cu(2) (Cu−N = 1.96−2.01 Å, Cu−Br = 2.36−2.48 Å), with the terminal Cu−Br distances significantly shorter than the bridging distances. Cu(1) and Cu(2) are juxtaposed with their metal planes roughly parallel, and long contacts between Cu(1) and Br(4) (2.899 Å) and Cu(2) and Br(2) (2.933 Å) may be considered to link them by weak axial interactions. Cu(1) and Cu(2) are displaced from the basal $N_2Br_2$ least-squares planes toward the apical bromines by 0.117 and 0.196 Å, respectively, in agreement with this suggestion. The copper ion ground state is therefore $d_{x2-y2}$ in both cases. The Cu(1)−Cu(2) distance is 3.670(1) Å. The Cu(1)−Cu(3) distance (3.269(1) Å) is substantially shorter than the Cu(2)−Cu(3) distances (4.163 Å) due to the much larger Cu−Br−Cu angle subtended at Br(4) (111.1° vs 82.7° at Br(2)). The charge balance in the complex indicates the presence of neutral PAH ligands in agreement with C−N distances (N(6)−C(12) = 1.28(1) Å, C(12)−N(7) = 1.31(1) Å, N(7)−N(8) = 1.44(1) Å), and it is apparent that the ligand exists in the imine tautomeric form.

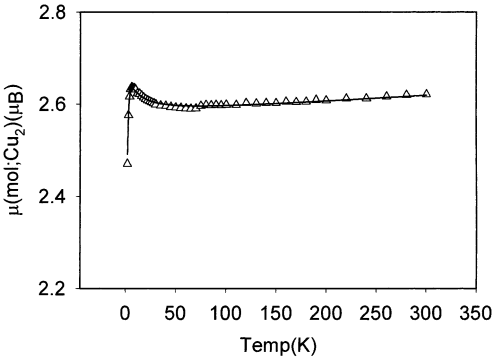


**Figure 2.** Magnetic moment per dinuclear copper(II) subunit in **1**. The solid line was calculated from the modified Bleaney−Bowers expression with $g = 2.102(8)$, $2J = 4.04(6)$ cm$^{-1}$, TIP = $90 \times 10^{-6}$ cm$^3$·mol$^{-1}$, $\Theta = -0.8$ K, and $\rho = 0$ ($10^2R = 0.33$).

**Magnetic Properties**. Magnetic data for **1** were collected as a function of temperature (2−300 K) in a 0.1 T field, and as a function of the field (0−5 T) at 2 K. Figure 2 shows a plot of magnetic moment per $Cu^{II}_2$ pair vs temperature. The magnetic moment decreases slightly from 300 to about 60 K, followed by an increase, and then a decrease below 7 K. Repeating the data collection and carefully calibrating the SQUID magnetometer with a typical Curie system showed that this behavior is real, and this suggests the presence of weak intramolecular ferromagnetic coupling, with a weaker antiferromagnetic component, evident at low temperature. A good fit of the data was obtained using the modified Bleaney−Bowers equation[27] (eq 1; $H = -2JS_1 \cdot S_2$), for $g =$

$$\chi_m = \frac{Ng^2\beta^2}{k(T-\Theta)}\left[\frac{1}{3+\exp(-2J/kT)}\right](1-\rho) + \left(\frac{Ng^2\beta^2}{4kT}\right)\rho + N\alpha \quad (1)$$

2.102(8), $2J = 4.04(6)$ cm$^{-1}$, $N\alpha = 90 \times 10^{-6}$ cm$^3$·mol$^{-1}$, $\rho = 0$, $\Theta = -0.8$ K ($10^2R = 0.33$) ($\Theta$ is a Weiss-like temperature correction, $N\alpha$ is temperature-independent paramagnetism, $\rho$ is the fraction of possible monomeric paramagnetic impurity, and $R = [\Sigma(\chi_{obsd} - \chi_{calcd})^2/\Sigma\chi_{obsd}^2]^{1/2}$). The solid line in Figure 2, expressed as magnetic moment per $Cu_2$ subunit, was calculated with these parameters. Figure 3 shows the magnetization data (per $Cu_2$ subunit) vs the field at 2 K, indicating that the system approaches saturation, but is not fully saturated at 5 T. The $N\beta$ value at 5 T (1.98) is consistent with a spin subunit with an $S = 2/2$ ground state, but the drop in moment at low temperature (Figure 2), signaling the presence of a longer range antiferromagnetic component, clearly contributes to the magnetization in this temperature range. However, these data support a weakly ferromagnetic system in agreement with the variable-temperature data, with a spin state approaching $S = 2/2$ for each half of the molecule.

Cu(1) and Cu(2) are juxtaposed with their magnetic orbitals roughly parallel, and separated by axial Cu−Br contacts of about 2.9 Å, leading to a nominally magnetically orthogonal situation. However, the magnetic orbitals could

(26) Haddad, S.; Willett, R. D. *Inorg. Chem.* **2001**, *40*, 809.

(27) Bleaney, B.; Bowers, K. D. *Proc. R. Soc. London, A* **1952**, *214*, 451.

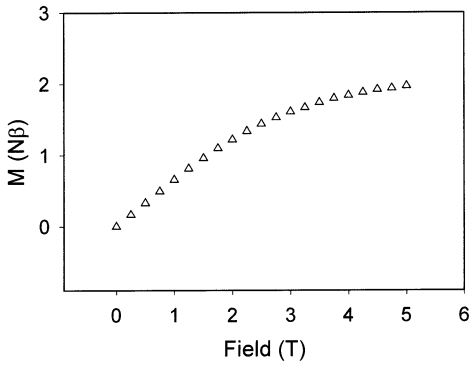


**Figure 3.** Magnetization data ($N\beta$) per dinuclear subunit for **1** at 2 K (0−5 T).

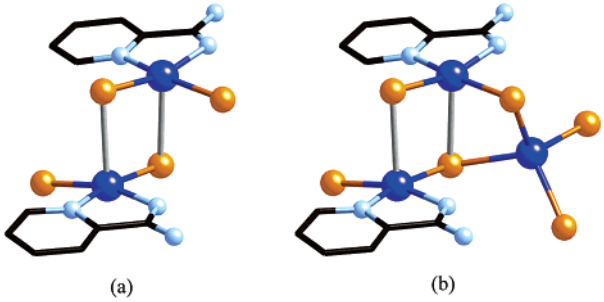


**Figure 4.** Dinuclear (a) and trinuclear (b, with $Zn^{II}$ replacing the tetrahedral $Cu^{I}$ atom) models used for the theoretical study.

be considered to have a rather weak $\delta$-type overlap involving only one lobe of each d orbital. Direct antiferromagnetic exchange between Cu(1) and Cu(2) would however be expected to be insignificant. The long four-bond, equatorial pathway via Cu(3) could possibly give rise to a weak antiferromagnetic component, although such exchange is not well documented through a $d^{10}$ $Cu^{I}$ ion. This would however be "absorbed" as part of the overall exchange between Cu(1) and Cu(2), which is weakly ferromagnetic. The negative $\Theta$ value reasonably results from a weak longer range interdinuclear antiferromagnetic exchange component, which may occur via the central $Cu^{I}_2Br_2$ core. However, an examination of the extended structure reveals a series of contacts between adjacent molecules (Br(2)′−Cu(2) = 4.539 Å, Br(4)′−Cu(1) = 4.682 Å) as they align in a stack in the "z" axis direction. This would seem to be a more viable intermolecular exchange route rather than the six-bond connection between dinuclear subunits within the same molecule. The weak ferromagnetic coupling can therefore be reasonably associated with the close proximity of Cu(1) and Cu(2), and a nonnegligible bridging interaction via their $d_{x2-y2}$ orbitals, through Br(2) and Br(4).

Density functional calculations for a simple dinuclear model complex (Figure 4a), including just bridging and terminal bromine atoms, consistently predict a ferromagnetic ground state with $2J = 5.3$ cm$^{-1}$, thus suggesting that each $Cu^{II}$ dinuclear unit in the hexanuclear compound is ferromagnetically coupled, but the two units connected through the $Cu^{I}_2Br_2$ core are essentially uncoupled. The ferromagnetic ground state must be attributed to the poor axial interaction of the bridging bromo ligands with the $d_{x^2-y^2}$ orbitals hosting the unpaired electrons, as seen by the small gap between the in-phase and out-of-phase combinations of those orbitals (1536 cm$^{-1}$). To put this value of the orbital gap in context, we may recall that the corresponding gap for a hydrogen-bonded dimer of $Cu^{II}$ in which the two Cu atoms are at a distance of 4.94 Å is roughly twice this value (3000 cm$^{-1}$)[28] and the experimental $2J$ value[29] is −94 cm$^{-1}$; the smaller gap in the present case accounts for a smaller antiferromagnetic contribution, whereas the shorter Cu···Cu distance (3.67 Å) is responsible for a stronger ferromagnetic contribution, resulting in the net ferromagnetic behavior observed ($2J_{calcd}$ = +5.3 cm$^{-1}$).

**Table 3.** Calculated Atomic Spin Populations for the Dinuclear $Cu_2$ and Trinuclear $Cu_2Zn$ Model Complexes (Figure 4)

| atom | dinuclear | trinuclear | atom | dinuclear | trinuclear |
|---|---|---|---|---|---|
| Cu(1) | 0.516 | 0.530 | N(2) | 0.069 | 0.084 |
| Cu(2) | 0.518 | 0.543 | N(5) | 0.082 | 0.097 |
| Br(1) | 0.153 | 0.145 | N(6) | 0.074 | 0.093 |
| Br(2) | 0.199 | 0.144 | Br(5) | | 0.006 |
| Br(3) | 0.197 | 0.157 | Br(6) | | 0.002 |
| Br(4) | 0.137 | 0.133 | Zn | | −0.001 |
| N(1) | 0.077 | 0.085 | | | |

Attempts at performing calculations for the trinuclear $Cu^{II}_2$-$Cu^{I}$ complex involving bridging and terminal bromine atoms (Figure 4b) were unsuccessful, with the calculations converging to a wave function with an unrealistic electron configuration. Good results were however obtained by substituting the bridging $Cu^{I}$ ion by the isoelectronic $Zn^{II}$ ion, whereby the calculated exchange coupling constant between the two $Cu^{II}$ atoms gave practically the same value as in the dinuclear model ($2J$ = 3.8 cm$^{-1}$). Such a result indicates that the magnetic behavior of our hexanuclear complex can be explained in terms of the interaction through the Br(4) and Br(2) atoms, without significant communication of the two dinuclear $Cu^{II}$ units through Cu(3) and Br(5).

The calculated spin density distribution (Table 3) shows that the largest spin population is located at the Cu atoms with significant delocalization toward the bridging and terminal ligands. The amount of spin delocalization to the Br atoms is nicely correlated to the Cu−Br distance: the largest populations (Br(2) and Br(3)) correspond to the shortest bonds, whereas the smallest population (Br(4)) is associated with the longest bond. The similar populations of Br(2) and Br(3) that present slightly different bond distances are probably due to the bridging nature of Br(2) compared to the terminal coordination of Br(3). The total spin density of the copper and the donor atoms amounts to 2.02, suggesting short-range spin delocalization. The addition of one tetrahedral $d^{10}$ ion in the trinuclear model results in only slight variations in the atomic spin densities, but the general spin distribution remains the same, and negligible spin density is transferred to the tetrahedral center (Zn, Br(5) and Br(6) atoms), consistent with the magnetically isolated character of the two $Cu^{II}$ dinuclear units as discussed above.

(28) Desplanches, C.; Ruiz, E.; Rodríguez-Fortea, A.; Alvarez, S. *J. Am. Chem. Soc.* **2002**, *124*, 5197.
(29) Bertrand, J. A.; Black, T. D.; Eller, P. G.; Helm, F. T.; Mahmood, R. *Inorg. Chem.* **1976**, *15*, 2965.

**Acknowledgment.** We thank the NSERC (Natural Sciences and Engineering Research Council of Canada) and Dirección General de Enseñanza Superior (DGES-Spain; Grant PB98-1166-C02-01) for financial support of this study.

**Supporting Information Available:** X-ray crystallographic file in CIF format for **1**. This material is available free of charge via the Internet at http://pubs.acs.org.

IC0204631